Published by IOP Publishing for Sissa Medialab

Received: *November 2, 2023*
Accepted: *February 12, 2024*
Published: *April 2, 2024*

Topical Workshop on Electronics for Particle Physics
Geremeas, Sardinia, Italy
1–6 October 2023

Performance of a novel charge sensor on the ion detection for the development of a high-pressure avalancheless ion TPC

Tianyu Liang,[a,b] **Dongliang Zhang,**[a,b,*] **Hulin Wang,**[a,b,*] **Chaosong Gao,**[a,b] **Jun Liu,**[a,b] **Xiangming Sun,**[a,b] **Le Xiao,**[a,b] **Feng Liu,**[a,b] **Bihui You,**[a,b] **Ling Liu,**[a,b] **Yichen Yang**[c] **and Kai Chen**[a,b,*]

[a] *PLAC, Key Laboratory of Quark & Lepton Physics (MOE), Central China Normal University, Wuhan, 430079, China*
[b] *Hubei Provincial Engineering Research Center of Silicon Pixel Chip & Detection Technology, Wuhan, 430079, China*
[c] *Institute of Modern Physics, Chinese Academy of Sciences, Lanzhou, 730000, China*

E-mail: dzhang@ccnu.edu.cn, hulin.wang@ccnu.edu.cn, chenkai@ccnu.edu.cn

Abstract: Within the project of building a time projection chamber using 100 kg of high-pressure $^{82}SeF_6$ gas to search for the neutrinoless double-beta decay in the NvDEx collaboration, we are developing a CMOS charge sensor, named Topmetal-S, which is tailored for the experiment to detect the ions without gas amplification. In this work, the performance of the sensor is presented. The equivalent noise charge of the sensor is measured to be about 120 to 140 e^- depending on the operating point, with the charge injection capacitance calibrated against external capacitors. The signal waveforms are investigated with various chip parameters and experimental settings. In addition to electrons, both negatively and positively charged ions could be detected, and their waveforms are studied using air and SF_6 gases. Using the sensor, the mobility of negative ions in ambient air in the atmospheric pressure is measured to be 1.555 ± 0.038 cm$^2 \cdot$ V$^{-1} \cdot$ s^{-1}. Our study demonstrates that the Topmetal-S chip could be used as the ion detection charge sensor for the experiment. Further work is ongoing to reduce the noise of the sensor and to develop a small readout plane with tens of the sensors.

Keywords: CMOS readout of gaseous detectors; Front-end electronics for detector readout; Gaseous imaging and tracking detectors; Time projection Chambers (TPC)

*Corresponding author.

https://doi.org/10.1088/1748-0221/19/04/C04004

Contents

2024 JINST 19 C04004

1 Introduction

The neutrinoless double-beta decay ($0\nu\beta\beta$), once observed, would have far-reaching implications in particle physics. It would confirm a lepton number violation process, demonstrate that neutrinos are Majorana fermions, and provide key information to understanding the origin of neutrino mass. We are embarking on a new $0\nu\beta\beta$ experiment called NvDEx [1], which uses high-pressure $^{82}SeF_6$ [2] gas in a time projection chamber (TPC). The intention is to exploit the tracking capability of the TPC, without compromising much on the energy resolution, to achieve a background-free search. Other $0\nu\beta\beta$ experiments based on gas TPC technique include NEXT [3] and PandaX-III [4].

Readout plane of CMOS charge sensors is envisaged to directly detect the drifting ions. The size of the charge sensor and its required noise level are studied using simulation [5]. During the first phase of the project with 100 kg of high-pressure $^{82}SeF_6$ gas, some 15000 sensors will be deployed in the readout plane [6]. In this paper, the performance of Topmetal-S [7], the charge sensor specifically designed for the NvDEx experiment, is presented.

2 Topmetal-S charge sensor

2.1 Chip architecture

The Topmetal-S sensor is fabricated in a 130 nm CMOS process. A photograph of the chip with wire-bonding board is shown in figure 1(a). It is 2.6 mm × 1.5 mm in size, mainly consisting of an exposed metal for sensing the drifting charges, and a charge-sensitive amplifier (CSA). The metal, named the charge collection electrode (CCE), has a hexagonal shape of 1 mm in diameter, surrounded by a guard ring. The operating point of the CSA can be adjusted via 6 bias voltages. The CSA converts the induced current into voltage waveforms, which are then digitized by an off-chip analog-to-digital converter (ADC). A focusing electrode is placed a few mm above the sensor to focus the electrostatic field onto the CCE. The structure of the focusing electrode and the small CCE without any transistors underneath, is to suppress the disturbance to the CCE caused by the in-chip circuits, so as to achieve better noise performance. A sketch of the charge sensing scheme is shown in figure 1(b).

Four variants of the sensors were produced in this second chip generation, mainly featuring different input transistor sizes and various feedback capacitors of CSA. The results in the paper are for one variant with relatively small noise. The design specifications of the sensor include a gain of 320 mV/fC, an equivalent noise charge (ENC) of 50 e^-, an input linear dynamic range of up to 35k e^-, a power consumption of 49.5 mW, and a maximum event rate per channel of about O(10) Hz.

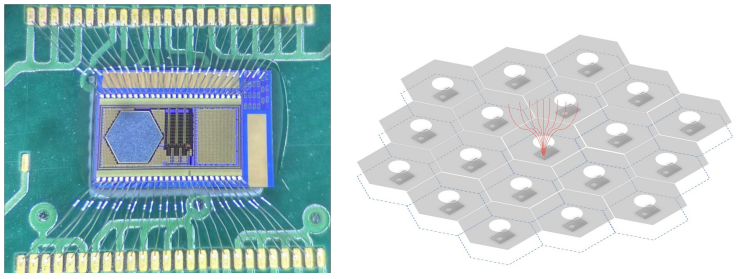

(a) (b)

Figure 1. (a) A photograph of one variant of the second generation of Topmetal-S sensors with wire-bonding board. The size of the sensor is 2.6 mm × 1.5 mm. (b) A sketch of the charge sensing scheme of the NvDEx experiment. Each readout channel has one Topmetal-S sensor placed below a focusing electrode.

2.2 Noise characterization

Currently, the noise of the sensor is characterized by its responses to the externally injected charges. The charge injection capacitor is formed by the CCE and its surrounding guard ring. It is found that its capacitance, both for the first and second-generation Topmetal-S chips, is much larger than what is extracted using the Calibre PEX tool, which leads to underestimated noise values reported earlier [5, 7].

The charge injection capacitance C_{gring} is now calibrated against external capacitors. As shown in figure 2(a), an external capacitor with known capacitance C_{ext} is wire-bonded to the CCE, thanks to CCE's large size. Pulses with different polarities, V_{ext} and V_{gring}, are injected simultaneously via C_{ext} and C_{gring}, respectively. The results are shown in figure 2(b). The mean of three measured C_{gring} values gives 255 ± 10 fF. The value is also roughly confirmed by a detailed simulation using the finite-element method with COMSOL [8] software.

The noise measurement of the Topmetal-S sensor is shown in figure 2(c). The ENC is measured to be 121 ± 9 e^-. The ENC shows no dependence on the size of injected charges up to ~40k e^-. It has a weak dependence on the discharge time provided that the discharge time is much longer than the rise time (~3 ms), increasing from 121 e^- to about 140 e^- as the τ_F decreases from 200 ms to 10 ms.

3 Performance on ion detection

3.1 Experimental setup

The experimental setup to evaluate the Topmetal-S sensor performance on ion detection is shown in figure 3. The apparatus includes a drift region defined by a field cage and an induction region defined by a focusing plane and a Topmetal-S sensor underneath. The field cage has a length of 19.9 cm and is formed by 2 cm × 1.6 cm copper strips of 1 mm width. The strips have a pitch of 2 mm and are connected using 10 MΩ resistors. An ^{241}Am α source with a collimator is placed right outside the field

2024 JINST 19 C04004

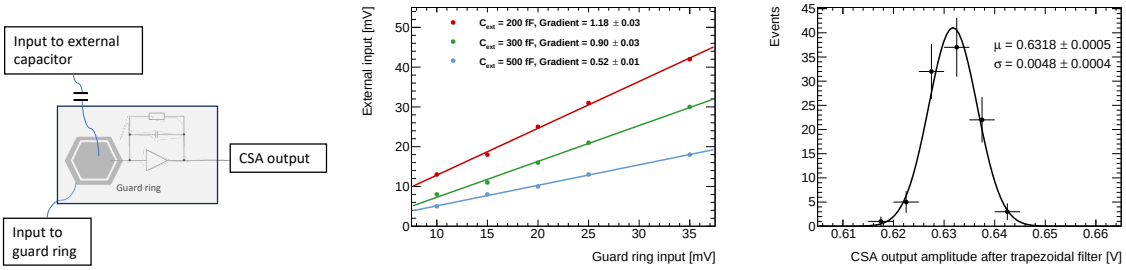

(a) (b) (c)

Figure 2. (a) Sketch of the measurement of charge injection capacitance by calibrating it against external capacitors. (b) The results of charge injection capacitance measurement using three external capacitances. (c) The distribution of amplitudes of CSA output waveforms after the trapezoidal filter, with a fixed charge injection of about 16k e^- for 100 times, and a discharge time constant of about 200 ms.

cage. A Passivated Implanted Planar Silicon (PIPS) detector with a sensitive area of 5 mm in diameter is used to detect the α particles, marking the initial time of the ionizing events. Output waveforms of both Topmetal-S sensor and PIPS detector are collected by an R&S RTM3004 oscilloscope. The apparatus is placed inside a gas-tight vessel with a length of 105 cm and an inner diameter of 20 cm. During the measurements, the pressure was around 1020 mbar and the temperature was around 297 K.

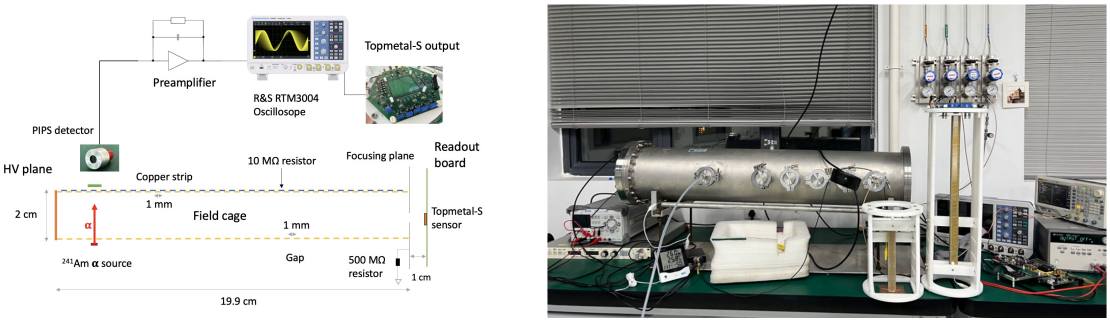

(a) (b)

Figure 3. (a) Schematic structure of the experimental setup. The drift region is defined by a field cage with a length of 19.9 cm. The induction region includes a Topmetal-S sensor beneath the focusing plane. (b) A photograph of the apparatus for measuring the Topmetal-S sensor performance.

3.2 Signal waveforms

The signal waveforms of the CSA of Topmetal-S are shown in figure 4. Figure 4(a) shows the waveforms of various discharge times and a fixed injected charge of about 8k e^-. The discharge time of the CSA of Topmetal-S can be practically tuned with τ_F ranging from ~3.5 ms to ~1.5 s. Figure 4(b) depicts the rising edge of the waveforms for α particles in Ar(90%)+CH_4(10%), ambient air, and SF_6 gases; the waveform for an injected pulse is also shown. The impact of the slow ion drift on the rise time is clearly seen in the waveforms. Figure 4(c) contains the average of 209 waveforms for α particles in SF_6 gas, for a drift field strength of 67 V/cm and drift length of 18.5 cm. No obvious minor peak is found in the waveform as discussed in ref. [9], and it will be further checked with longer drift distances of up to 50 cm. The waveform of positive ions in ambient air is shown in figure 4(d).

2024 JINST 19 C04004

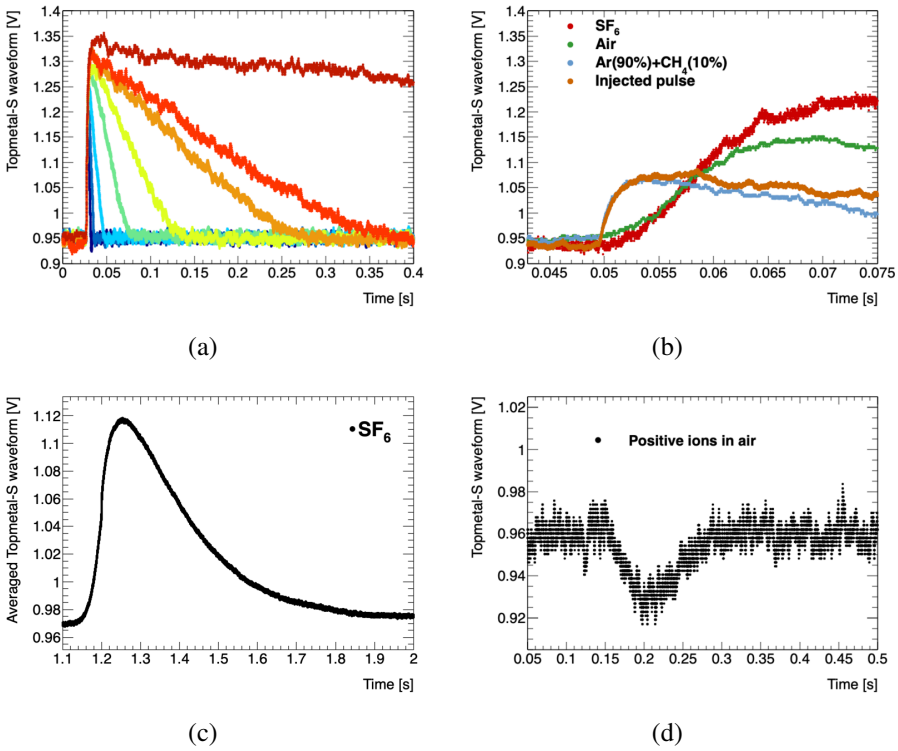

Figure 4. The signal waveforms of the CSA of Topmetal-S. (a) The waveforms with discharge time constant ranging from ~3.5 ms to ~1.5 s and a fixed injected charge of about 8k e^-. (b) The rising edge of the waveforms for α particles in various gases and for an injected pulse. (c) The average of 209 waveforms for α particles in SF_6 gas. (d) The waveform of positive ions for α particle in ambient air.

3.3 Drift velocity measurement

The drift velocities of negative ions in ambient air are measured with Topmetal-S sensor. For each specific drift field, the α source is positioned at 4 different drift distances ranging from 4 cm to 18.5 cm. The drift velocity is measured for 5 electric field strengths ranging from 50 V/cm to 200 V/cm.

The drift time distributions for a fixed drift field of 100 V/cm and a fixed drift length of 9 cm are shown in figure 5(a) and 5(b), respectively. Since the number of recorded events varies between ~60 to ~300 for each measurement, each drift time distribution is normalized according to the number of events in a ±2 ms window around its peak.

The average drift time as a function of drift distance for various drift field strengths is presented in figure 6(a). The measured drift velocity as a function of drift field strength is shown in figure 6(b). The mean measured mobility is 1.555 ± 0.038 $cm^2 \cdot V^{-1} \cdot s^{-1}$. Its uncertainty is calculated as the standard deviation of the measured mobilities at different drift field strengths.

The measurements are dominated by the systematic uncertainties. One probable main source is the fluctuations in the local pressure, temperature, and gas composition, especially the humidity level in the ambient air. Another probable main source is the distortion of the drift field near the end plates of the field cage, which we are improving on. Besides, the results suffer from the α particles that don't reach the PIPS detector, due to the poor quality of the ^{241}Am source retrieved from a smoke detector. In addition, there are fake signals induced by the high-voltage system on the PIPS detector and the Topmetal-S sensor, which need to be suppressed in the large system.

2024 JINST 19 C04004

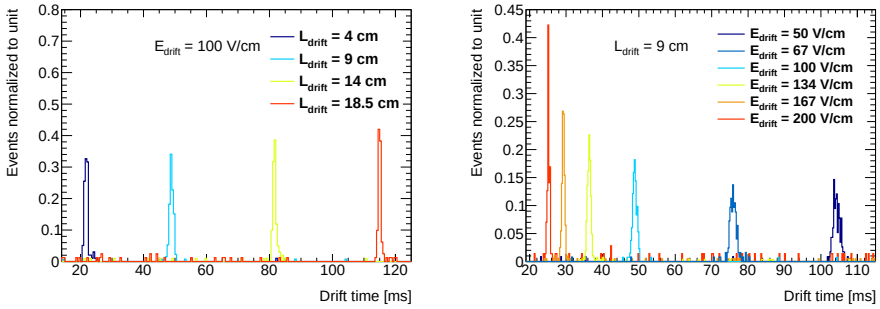

(a) (b)

Figure 5. The drift time distributions for various drift lengths (a), and various drift field strengths (b). Each drift time distribution is normalized according to the number of events in a ±2 ms window around its peak. The uncertainties shown are statistical only.

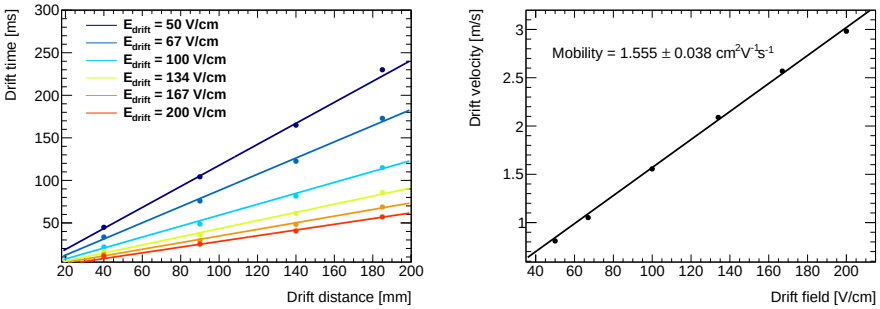

(a) (b)

Figure 6. (a) The average drift time as a function of the drift distance for various drift field strengths. (b) The drift velocity as a function of drift field strength. The uncertainties shown are statistical only.

4 Conclusion

The performance of the second-generation Topmetal-S charge sensor specifically designed for the NvDEx experiment is presented. The discharge time of the CSA of sensor can be practically tuned with τ_F ranging from ~3.5 ms to ~1.5 s. The rise time of the waveform is ~3 ms for injected pulses. The ENC of the sensor varies between ~ 120 to ~ 140 e^- depending on the operating point. The signal waveforms for electrons, positively and negatively charged ions are studied with a small TPC and an ^{241}Am α source in Ar(90%)+CH_4(10%), ambient air, and SF_6 gases. The drift velocities of the negatively charged ions in ambient air are measured with the Topmetal-S sensor. The measured ion mobility is 1.555 ± 0.038 cm$^2 \cdot$ V$^{-1} \cdot$ s^{-1}, with the uncertainty dominated by systematic sources.

The results obtained support the use of the Topmetal-S sensor for the NvDEx experiment. Further development of the sensor is ongoing. A small readout plane with tens of the sensors is being constructed to further characterize the tracking capability and energy resolution of the readout scheme.

Acknowledgments

This work was supported in part by the National Natural Science Foundation of China under Grant 12105110, and in part by the National Key Research and Development Program of China under Grant 2022YFA1604703.

2024 JINST 19 C04004

References

[1] NνDEx-100 collaboration, *NvDEx-100 conceptual design report*, *Nucl. Sci. Tech.* **35** (2024) 3 [arXiv:2304.08362].

[2] D.R. Nygren et al., *Neutrinoless Double Beta Decay with $^{82}SeF_6$ and Direct Ion Imaging*, 2018 *JINST* **13** P03015 [arXiv:1801.04513].

[3] NEXT collaboration, *Sensitivity of a tonne-scale NEXT detector for neutrinoless double beta decay searches*, *JHEP* **08** (2021) 164 [arXiv:2005.06467].

[4] X. Chen et al., *PandaX-III: Searching for neutrinoless double beta decay with high pressure ^{136}Xe gas time projection chambers*, *Sci. China Phys. Mech. Astron.* **60** (2017) 061011 [arXiv:1610.08883].

[5] Y. Mei, X. Sun and N. Xu, *Topmetal CMOS direct charge sensing plane for neutrinoless double-beta decay search in high-pressure gaseous TPC*, arXiv:2010.09226.

[6] L. Lang et al., *Design and Demonstration of Digital Readout Chain in NvDEx Experiment*, *IEEE Trans. Nucl. Sci.* **70** (2023) 2499.

[7] C. Gao et al., *A Low-Noise Charge-Sensitive Amplifier for Gainless Charge Readout in High-Pressure Gas TPC*, *PoS* **TWEPP2018** (2019) 083.

[8] COMSOL, Inc., *COMSOL — Software for Multiphysics Simulation*, (2022), https://www.comsol.com.

[9] N.S. Phan et al., *The novel properties of SF_6 for directional dark matter experiments*, 2017 *JINST* **12** P02012 [arXiv:1609.05249].

2024 JINST 19 C04004